YAŞAR UNIVERSITY

GRADUATE SCHOOL

MASTER OF SCIENCE THESIS

BINARY SIGNAL RECOVERY IN EXTREME UNDERSAMPLING: SDP WITH MAJORITY VOTING AND SUCCESIVE INTERFERENCE CANCELLATION

ECE ABAY

THESIS ADVISOR: ASSOC.PROF.(PHD) BURHAN GÜLBAHAR

MSC IN ELECTRICAL AND ELECTRONICS ENGINEERING

BORNOVA / İZMİR
AUGUST 2025

JURY APPROVAL PAGE

We certify that, as the jury, we have read this thesis and that in our opinion it is fully adequate, in scope and in quality, as a thesis for the degree of Master in Science.

Jury Members:	**Signature:**
Assoc. Prof. (PhD) Burhan GÜLBAHAR Yaşar University	.....
Prof. (PhD) Olcay AKAY Dokuz Eylül University	.....
Assoc. Prof. (PhD) Nalan ÖZKURT Yaşar University	.....

Prof. (PhD) Yücel Öztürkoğlu
Director of the Graduate School

ABSTRACT

BINARY SIGNAL RECOVERY IN EXTREME UNDERSAMPLING: SDP WITH MAJORITY VOTING AND SUCCESSIVE INTERFERENCE CANCELLATION

Abay, Ece
MSc, Electrical and Electronics Engineering
Advisor: Assoc. Prof. (PhD) Burhan GÜLBAHAR

August 2025

Binary compressive sensing (BCS) addresses the challenge of recovering a k-sparse binary vector of length n from m linear measurements, where $m \ll n$. In the extreme undersampling regime ($m < 2k$), traditional compressive sensing (CS) guarantees breakdown, and existing BCS algorithms with random sensing matrices exhibit suboptimal performance. This paper introduces SDP-MVRSIC, a novel algorithm that integrates semidefinite programming (SDP), majority voting (MV), and recursive successive interference cancellation (SIC) to achieve reliable recovery even when $m \leq k$. The method employs a recursive tree structure with $L \ll n$ SIC layers, where each node generates candidate solutions via randomized SDP sampling, refine them using MV, and propagates branches for subsequent SIC stages. The cost function $C(\hat{\boldsymbol{x}}) = \|\boldsymbol{y} - \boldsymbol{H}\hat{\boldsymbol{x}}\|_2^2$ guides the selection of optimal candidates.

SDP-MVRSIC offers a tunable trade-off between computational complexity and recovery accuracy. For instance, when $n = 128$, increasing the complexity from $O(n^{3.83})$ to $O(n^{5.86})$ enables exact recovery for $m/k \in [0.6, 1.5]$ as the sparsity ratio $s = k/n$ decreases from 0.5 to 0.125. This flexibility makes the algorithm particularly suited for applications with stringent measurement constraints, such as overloaded MIMO systems or resource-limited sensor networks.

Keywords: binary compressed sensing, SDP, majority voting, successive interference cancellation

ÖZ

AŞIRI AZ ÖRNEKLEMEDE İKİLİ SİNYAL KURTARMA: ÇOĞUNLUK OYLAMASI VE ARDIŞIK GİRİŞİM İPTALİ İLE BİRLİKTE SDP

Abay, Ece
Yüksek Lisans Tezi, Elektrik Elektronik Mühendisliği
Danışman: Doç. Dr. Burhan GÜLBAHAR

Ağustos 2025

İkili Seyrek Algılama (BCS), n uzunluğundaki k-seyrek bir ikili vektörün m doğrusal ölçümden ($m \ll n$) kurtarılması problemini ele alır. Aşırı örnekleme eksikliği rejiminde ($m < 2k$), geleneksel seyrek algılama (CS) garantileri geçerliliğini yitirir ve rastgele ölçüm matrisleri kullanan mevcut BCS algoritmaları yetersiz performans sergiler. Bu makale, $m \leq k$ durumunda bile güvenilir kurtarma sağlamak için yarı-tanımlı programlama (SDP), çoğunluk oylaması (MV) ve özyinelemeli ardışık girişim iptali (SIC) tekniklerini birleştiren SDP-MVRSIC adlı yeni bir algoritma sunmaktadır. Yöntem, $L \ll n$ SIC katmanına sahip özyinelemeli bir ağaç yapısı kullanır. Her düğüm, rastgele SDP örneklemesiyle aday çözümler üretir, bunları MV ile rafine eder ve sonraki SIC aşamaları için dallar oluşturur. $C(\hat{\boldsymbol{x}}) = \|\boldsymbol{y} - \boldsymbol{H}\hat{\boldsymbol{x}}\|_2^2$ maliyet fonksiyonu, en uygun adayların seçimine rehberlik eder.

SDP-MVRSIC, hesaplama karmaşıklığı ve kurtarma doğruluğu arasında ayarlanabilir bir denge sunar. Örneğin, $n = 128$ için karmaşıklığın $O(n^{3.83})$'ten $O(n^{5.86})$'ya çıkarılması, seyreklik oranı $s = k/n$ 0.5'ten 0.125'e düştükçe $m/k \in [0.6, 1.5]$ aralığında tam kurtarma sağlar. Bu esneklik, algoritmayı aşırı yüklenmiş MIMO sistemleri veya kaynak kısıtlı sensör ağları gibi zorlayıcı ölçüm kısıtlamaları olan uygulamalar için özellikle uygun hale getirir.

Anahtar Kelimeler: ikili seyrek algılama, yarı-tanımlı programlama, çoğunluk oylaması, ardışık girişim iptali

ACKNOWLEDGEMENTS

I am profoundly grateful to my thesis advisor, Assoc. Prof. Burhan GÜLBAHAR, whose expertise was invaluable in formulating the research questions and methodology. His insightful feedback pushed me to sharpen my thinking and brought my work to a higher level.

I extend my sincere thanks to the members of my thesis committee, Prof. Olcay AKAY and Assoc. Prof. Nalan ÖZKURT, for their time, insightful comments, and challenging questions which greatly contributed to the quality of this work.

The numerical simulations were partially performed at TUBITAK ULAKBIM High Performance and Grid Computing Center. I gratefully acknowledge this support.

Words cannot express my gratitude to my beloved family; my parents, Hanife and Mehmet, and my brother, Efe, for their unconditional love, endless support, and belief in me throughout my life. This accomplishment would not have been possible without them.

Last but certainly not least, I would like to thank my better half, Burak, for his incredible patience, understanding, and endless encouragement throughout this challenging process. This thesis is as much his as it is mine.

Ece Abay

İzmir, 2025

TEXT OF OATH

I declare and honestly confirm that my study, titled “BINARY SIGNAL RECOVERY IN EXTREME UNDERSAMPLING: SDP WITH MAJORITY VOTING AND SUCCESSIVE INTERFERENCE CANCELLATION” and presented as a Master’s Thesis, has been written without applying any assistance inconsistent with scientific ethics and traditions. I declare, to the best of my knowledge and belief, that all content and ideas drawn directly or indirectly from external sources are indicated in the text and listed in the list of references.

Ece Abay

26.08.2025

TABLE OF CONTENTS

LIST OF FIGURES

LIST OF TABLES

SYMBOLS AND ABBREVIATIONS

SYMBOLS:

Δ	Sparsity tolerance factor
C($\hat{\boldsymbol{x}}$)	Cost function
H	Measurement matrix
k	Sparsity level
L	Number of SIC layers
m	Number of measurements
n	Signal length
N_m	Lowest-cost strings
N_s	Random sample vectors
s	Sparsity ratio
x	Binary sparse signal
y	Measurement vector

ABBREVIATIONS:

AL0	Approximated l_0 norm
BCS	Binary compressed sensing
CRUS	Cost-restricted uniform sampling
CS	Compressed sensing
DCT	Discrete cosine transform
LP	Linear programming
MIMO	Multiple-Input Multiple-Output
ML	Maximum Likelihood
MMSE	Minimum mean-squared error

NP hard	Non-deterministic polynomial hard
OMP	Orthogonal matching pursuit
POP	Polynomial optimization problem
QAOA	Quantum approximate optimization algorithm
RIP	Restricted isometry property
RWR	Reweighted l_1 minimization
SDP	Semidefinite programming
SDP-MVRSIC	SDP with MV and recursive SIC
SIC	Successive interference cancellation
SNR	Signal-to-Noise Ratio
SSIM	Structural SIMilarity index
UASN	Underwater wireless sensor networks
UWSN	Underwater acoustic sensor network

1. CHAPTER: INTRODUCTION

The emergence of compressive sensing (CS) has revolutionized in signal acquisition and processing. CS theory fundamentally differs from the Nyquist-Shannon sampling rule that requires sampling at twice the maximum frequency of the signal, demonstrating that sparse signals can be perfectly reconstructed from significantly fewer linear measurements. This groundbreaking approach has profound implications for applications where traditional sampling methods are impractical due to resource constraints or time limitations.

The theoretical foundations of CS were established through two landmark publications in 2006. Seminal work “Compressed Sensing” written by D. L. Donoho (2006) and "Robust Uncertainty Principles: Exact Signal Reconstruction from Highly Incomplete Frequency Information" published by E. J. Candès et al. (2006), mathematically demonstrated that sparse signals could be exactly recovered through optimization techniques using measurement counts substantially below the signal dimension.

One of the important theoretical advances in CS is the introduction of the Restricted Isometry Property (RIP) by E. J. Candès et al. (2005). The fact that the measurement matrix satisfies the RIP property condition largely guarantees the recovery of the sparse signal.

The core CS problem can be formally stated as the reconstruction of a sparse signal vector $\boldsymbol{x} \in \mathbb{R}^n$ from undersampled measurements $\boldsymbol{y} = \boldsymbol{H}\boldsymbol{x}$, where $\boldsymbol{H} \in \mathbb{R}^{mxn}$ $(m \ll n)$ represents the measurements matrix. This underdetermined problem typically addressed through l_1-norm minimization proposed by E. J. Candès et al. (2006):

$$\min_{\boldsymbol{x}} \|\boldsymbol{x}\|_1 \text{ subject to } \boldsymbol{y} = \boldsymbol{H}\boldsymbol{x} \tag{1}$$

The practicality of CS originates the inherent sparsity of many natural signals when represented in appropriate domains (e.g., wavelet or Fourier bases). This sparsity enables the development of efficient acquisition strategies combining random measurement schemes with reconstruction algorithms such as Basis Pursuit proposed

by S. S. Chen et al. (1998), iterative reweighted l_1-minimization published by E. J. Candès et al. (2008).

While traditional CS focuses on real-valued signals, numerous practical applications in digital communication and data processing require recovery of binary-valued signals ($\{0, 1\}$ or $\{-1, 1\}$). This necessity has given rise to new problem called binary compressed sensing (BCS) with paper named "Recovery thresholds for l_1 optimization in binary compressed sensing" written by M. Stojnic (2010) and "BCS: Compressive sensing for binary sparse signals" published by U. Nakarmi et al. (2012).

The rest of this study is organized as follows: Chapter 2 presents the binary compressive sensing (BCS), Chapter 3 gives the literature review, and Chapter 4 explains proposed SDP-MVRSIC reconstruction algorithm for BCS under four main steps. Chapter 5 includes explanation of proposed SDP with sparse measurements algorithm. Chapter 6 discusses computational complexity of SDP-MVRSIC algorithm. Chapter 7 shows numerical simulations in both exact recovery performance and bit error rate performance of the algorithm to evaluate the success of the SDP-MVRSIC. Chapter 8 gives the conclusion and direction for future work on this subject.

2. CHAPTER: BINARY COMPRESSED SENSING (BCS)

In the noiseless setting of Binary Compressed Sensing (BCS), the core objective is to reconstruct a sparse binary signal $\boldsymbol{x}$ (where each component satisfies $x_i \in \{0,1\}$ or $\{-1,1\}$) from a limited set of linear measurements:

$$\boldsymbol{y} = \boldsymbol{H}\boldsymbol{x} \tag{2}$$

Here, $\boldsymbol{H} \in \mathbb{R}^{mxn}$ denotes the measurement matrix with $m \ll n$, and $\boldsymbol{y} \in \mathbb{R}^m$ represents the observed measurement vector. The measurement matrix $\boldsymbol{H}$ is said to satisfy the Restricted Isometry Property (RIP), introduced by Candès E. J. et al. (2005), of order k with constant $\delta_k \in (0,1)$ if for all k-sparse vectors $\boldsymbol{x}$, the following inequality holds:

$$(1 - \delta_k)\|\boldsymbol{x}\|_2^2 \leq \|\boldsymbol{H}\boldsymbol{x}\|_2^2 \leq (1 + \delta_k)\|\boldsymbol{x}\|_2^2 \tag{3}$$

Random matrices with entries drawn independently from Gaussian or Bernoulli distributions are widely known to satisfy the RIP with high probability, which makes them particularly suitable for compressed sensing applications. This fundamental result, introduced in studies by E. J. Candès et al. (2005), R. Baraniuk et al. (2008), and D. L. Donoho (2006), supports the use of random matrices in sparse signal recovery and has played a central role in the theoretical development of compressed sensing.

BCS problems are defined by two fundamental properties: sparsity and discreteness. A signal $\boldsymbol{x}$ is called k-sparse if it has no more than k non-zero elements; this property is also valid for classical compressed sensing. However, the problem gets more complex when each non-zero element x_i must take a binary value (e.g., $x_i \in \{-1,1\}$), turning it into a mixed-integer optimization problem which is NP-hard.

This discrete-valued signal has been studied by Z. Hajji et al.'s (2020) and R. Hayakawa et al.'s (2017) and can be seen in many other real-world applications such as massive multiple input multiple output systems where signal has binary characteristics. Unlike conventional compressed sensing, which deals with continuous-valued sparse signals, BCS introduces computational and theoretical

challenges due to the non-convexity imposed by binary constraints. The binary constraint not only complicates the reconstruction process but also raises fundamental questions about the minimum number of measurements m required for exact recovery and the design of efficient algorithms capable of handling this conbinatorial optimization problem. Addressing these questions forms the motivation behind the development of BCS algorithms such as the one proposed in this study.

3. CHAPTER: LITERATURE REVIEW

The literature review is divided into four categories. First category examines the state-of-the-art algorithms related to BCS. Next category is focused on Semidefinite Programming (SDP) based signal recovery methods. In third category, application of Majority Voting-Successive Interference Cancellation on signal processing are discussed. Final category is about current algorithms which are used in extreme under sampling regimes and their challenges.

3.1. The State-of-the-art Algorithms for BCS

This section focused on four important studies that have contributed the development of Binary Compressed Sensing (BCS). First, we discuss M. Stojnic's (2010) theoretical analysis of l_1 optimization for binary signals, which established foundational recovery guarantees. In following paper written by U. Nakarmi et al. (2012), we investigate bipartite graph framework which introduced a combinatorial approach to BCS. Then we analyze S. Sparrer et al.'s (2016) MMSE-based OMP algorithm. As a final study, we examine S. M. Fosson's (2018) non-convex optimization method, which takes advantage of iterative reweighting.

In M. Stojnic (2010)'s article, he tried to recover binary sparse signals using l_1 optimization. Unlike classical CS algorithms, he exploited the property that binary signals belong to a set of two elements, meaning that if they are nonzero, they are 1, and if they are zero, they are 0. The author modifies the standard l_1 optimization problem by introducing constraints that bound the solution to the interval $[0,1]$. This modification exploits the binary nature of the signal, enabling higher recoverable sparsity thresholds compared to generic non-negative sparse signals. The theoretical analysis is grounded in a probabilistic framework, assuming the measurement matrix $\boldsymbol{H}$ has null-space uniformly distributed in the Grassmanian, which simplifies the derivation of performance bounds.

A central contribution of the paper is the derivation of the weak threshold βw, which quantifies the maximum sparsity level $k = \beta w n$ that can be recovered with

overwhelming probability for a given number of measurements $m = \alpha n$. The analysis builds on Gordon's "escape through a mesh" theorem and introduces functions f_1, f_2, and f_3 to bound the probability of successful recovery. The results demonstrate that binary signals achieve higher recoverable sparsity than general non-negative signals, particularly as $\alpha \to 0.5$, where $\beta w/\alpha \to 1$. This implies that binary signals require at most $m = n/2$ measurements for exact recovery, regardless of sparsity—a significant improvement over conventional CS.

This paper provides a theoretical foundation for binary compressed sensing, offering both analytical insights and empirical validation that advance the field beyond generic sparse recovery techniques. However, one notable limitation of Stojnic's work is the absence of a thorough investigation into the regime where $k > m$—that is, when the sparsity level exceeds the number of measurements. While the paper establishes strong recovery guarantees for $k \leq m$, it does not explore whether the proposed l_1 optimization with binary constraints remains effective in highly underdetermined scenarios where k significantly surpasses m. This gap leaves open questions about the algorithm's robustness in extreme sparsity regimes. On the other hand, the paper's numerical experiments empirically validate recovery thresholds but omit runtime measurements or scalability comparisons.

U. Nakarmi et al. (2012) proposed a novel bipartite graph framework for BCS, addressing limitations of conventional l_1-based methods. Their approach designs a sparse measurement matrix ϕ with a Unique Sum Property (each row's non-zero elements' sums are distinct), enabling binary recovery via a three-phase decoding algorithm:

- First Phase Recovery identifies deterministic nodes (Zero/Light Check Nodes),
- Edge Removal iteratively simplifies the graph,
- Check Sum Method resolves ambiguities in Heavy Check Nodes using combinatorial search.

Simulations demonstrate low error rates ($\sim 10^4$ at 25% sampling) and faster decoding than l_1 methods, adhering to the theoretical bound error rate = $\left(1 - \frac{L}{N}\right)^M$. L is non-zero entries per row in measurement matrix tested at L = 20-30, N is signal length ($N = 1000$ for this study) and M represents number of measurements which were 200-300 for sampling rates $S.R. = M/N$ = 0.2-0.3. Their method avoids complex optimization,

achieving faster reconstruction than traditional l_1-based approaches, particularly for moderately sparse signals. However, this approach is limited to sparse measurement matrices, making it unsuitable for applications requiring dense matrices. Additionally, the graph-theoretic formulation lacks the geometric intuition of conventional CS, which relies on properties like RIP for theoretical guarantees. Despite these limitations, graph-based BCS can be effective in resource-constrained applications (e.g., IoT, sensor networks), where sparse matrices reduce computational and hardware complexity.

S. Sparrer et al. (2016) proposed an enhanced version of the traditional compressed sensing approach Orthogonal Matching Pursuit (OMP) algorithm introduced by Y.C. Pati et al. (1993), replacing Zero Forcing (ZF) criterion with Minimum Mean-Squared Error (MMSE) to improve performance over the noisy binary measurements.

This algorithm significantly improves reconstruction accuracy, particularly in high Signal-to-Noise Ratio (SNR) regimes, achieving a performance gain of over 1 dB compared to the conventional ZF-OMP.

Unlike ZF-OMP, which uses the Moore-Penrose pseudoinverse for signal estimation, MMSE-OMP employs a modified equalization matrix:

$$A_I^{(M)} = X_S A_S^T \left(A_S X_S A_S^T + A_{\bar{S}} X_{\bar{S}} A_{\bar{S}}^T + \sigma_n^2 I \right)^{-1}, \quad (4)$$

where X_S and $X_{\bar{S}}$ are diagonal matrices which refer to the variances of detected and undetected symbols, respectively. This formulation explicitly models the interference from undetected non-zero elements, a feature absents in ZF-OMP.

Further, the authors address the bias introduced by MMSE estimation by scaling the estimated signal with a diagonal matrix $C = diag\left(\frac{1}{B_{1,1}}, \dots, \frac{1}{B_{E,E}}\right)$, where $B = A_I^{(M)} A_S$. The paper also introduces practical approximations for the variances $\sigma_{X_S}^2$ and $\sigma_{X_{\bar{S}}}^2$, leveraging binary symbol priors to reduce computational complexity. For instance, elements with estimated magnitudes greater than 0.5 are assumed correct, while others are treated as erroneous.

While the MMSE-OMP algorithm demonstrates notable improvements in high-SNR regimes, its evaluation is limited to scenarios with relatively low sparsity (e.g. $k = 20$, $n = 258$, where k is the number of non-zero elements of the signal and n represents

length of the signal) and a generous measurement ratio ($m = 129,\ 50\%\ of\ n$). This contrasts sharply with an extreme undersampling setting.

S. M. Fosson (2018) introduced a non-convex optimization framework for binary compressed sensing by designing a tailored cost functional:

$$F(x) = \frac{1}{2}\|y - Ax\|_2^2 + \lambda \sum_{i=1}^{n} \left(x_i - \frac{1}{2}x_i^2\right), \tag{5}$$

which enforces binary constraints with a concave penalty $g(x) = \sum_i \left(x_i - \frac{1}{2}x_i^2\right)$. The proposed iterative reweighting (RW) algorithm iteratively minimizes this functional through alternating weight updates and Lasso steps, solved via ADMM. While this approach demonstrates superior exact recovery rates compared to classical convex methods like standard Lasso or Basis Pursuit (achieving 100% success at $m = 25$ measurements for sparsity $k = 5$), its performance heavily depends on careful initialization. To mitigate this, the author proposes the RWR variant -a multi start strategy that restarts RW from random points upon failure- which empirically improves robustness but lacks theoretical convergence guarantees. This study, as the previous work examined, does not evaluate the algorithm's performance under conditions of extreme under sampling, where the number of measurements m is significantly lower than the sparsity level k. While proposed non-convex approach demonstrates promising results for $m \geq 25$ with $k = 5 (m \approx 5k)$, it remains untested in more challenging regimes where $m < 2k$ or when dealing with higher sparsity ratios ($k/n > 0.1$).

The recovery of binary sparse signals from compressed measurements has evolved through diverse methodological approaches, each addressing unique challenges. M. Stojnic (2010) laid the theoretical groundwork by adapting l_1 optimization with $[0,1]^n$ constraints, demonstrating improved sparsity thresholds for binary signals but leaving the $k > m$ regime unexplored. U. Nakarmi et al. (2012) introduced a graph-based framework based on Unique Sum Property. This framework decoded signals from sparse measurement matrices but did not satisfy RIP property. S. Sparrer et al. (2016) were able to recover binary signals by improving OMP via MMSE estimation, but this method required large number of measurements ($m/n = 0.5$). S. M. Fosson (2018) combined non-convex optimization and iterative reweighting. Her algorithm

performed well at moderate sparsity ($m \approx 5k$), however was unstable in extreme undersampling situtations. In summary, critical blanks of their studies were theoretical explanation, computational complexity analysises, and scalability of their works to $k > m$. We aimed to address these open points in our study.

3.2. Semidefinite Programming (SDP)-Based Signal Recovery Methods

While convex relaxation approaches are very common in BCS literature, SDP-based approaches are mathematically convenient for recovering binary sparse signals by using polynomial optimization. S. M. Fosson et al. (2019) proposed an algorithm with reformulating BCS problem as a polynomial optimization problem (POP). The key idea involves minimizing the non-convex objective function $\sum_{i=1}^{n}(x_i - x_i^2)$ subject to the linear constraints $\boldsymbol{y} = \boldsymbol{Hx}$, where $\boldsymbol{x} \in [0,1]^n$. This formulation ensures that global minima lie in the binary set $\{0,1\}^n$. Thus, it recovers the binary sparse signal under a single solution. Authors claim that a first-order relaxation is enough to reach the global optimum. And they demonstrated that they could solve the problem using SDP relaxations.

However, because solving the SDP relaxation in large-scale problems (larger n) increases computational complexity, the authors divided the problem into smaller subproblems. To this end, they took advantage of the chordal sparsity property. They added slack variables to the problem and adjusted constraints. Thus, they succeeded in reducing computational complexity.

In the paper, they also improve proposed method for noisy measurements. They transform $\boldsymbol{y} = \boldsymbol{Hx}$ constraint into $\|\boldsymbol{Hx} - \boldsymbol{y}\|_\infty \leq \eta$ constraint by adding noise parameter. Authors emphasize that a solution is found for low noisy measurements, while maintaining the robustness of their method.

Numerical simulations were conducted to validate the effectiveness of the proposed approach. The experiments considered binary signals of dimension $n = 100$ with varying sparsity levels k and measurement counts m. The results demonstrated superior performance compared to state-of-the-art methods, particularly in scenarios with moderate to high sparsity. However, S. M. Fosson et al.'s (2019) numerical experiments primarily focused on scenarios where the sparsity level k was smaller than or comparable to the number of measurements m (e.g., $k \leq 15\ for\ m = 45$).

While their results are compelling for $k \ll m$, the performance for highly underdetermined systems ($k > m$) remains underexplored—a gap our work explicitly targets. Our simulations extend their analysis to this challenging regime, demonstrating robust recovery even when the signal's sparsity exceeds measurements. This advancement not only complements their contributions but also broadens the applicability of SDP-based methods in extreme under sampling scenarios.

3.3. Application of Majority Voting-Successive Interference Cancellation (MVSIC) on Signal Processing

The integration of Majority Voting (MV) and Successive Interference Cancellation (SIC) methods, collectively known as MVSIC, has emerged as a transformative approach in signal processing, particularly for sparse signal reconstruction problems. This methodology bridges quantum computing and classical signal processing techniques, offering innovative solutions to the persistent challenges of computational complexity versus accuracy trade-offs in traditional methods. The QAOA-MVSIC method developed by B. Gulbahar (2025) aims to improve maximum-likelihood (ML) detection in massive multiple-input multiple-output (MIMO) systems using the Quantum Approximate Optimization Algorithm (QAOA). The study addresses the increasing errors due to increased circuit depth and problem size, as well as the challenges of Noisy Intermediate-Scale Quantum (NISQ) devices. QAOA-MVSIC method combines recursive QAOA (RQAOA), majority voting (MV) and successive interference cancellation (SIC) to increase feasibility and performance. B. Gulbahar (2025) achieves near-optimal bit error rate (BER) at low complexity by recursively reducing problem size in his algorithm. He demonstrates this through simulations and experiments on IBM quantum processors.

The research begins by emphasizing the limitations of QAOA in large-scale MIMO systems due to noise and gate errors in NISQ devices. To avoid these issues, author changes RQAOA by implementing cost sorting and final selection operations in fewer steps and by doing this he reduces the quantum circuit depth. The integration of MV and SIC further improves robustness against noise, enabling partial decoding and interference cancellation. Simulations for 24×24 and 12×12 MIMO systems with binary and quadrature phase-shift keying (BPSK/QPSK) modulations show that

QAOA-MVSIC achieves near-optimal performance with a shallow circuit depth of ($p = 1$) and a small number of steps ($m \leq 4$).

A key innovation of the work is the truncation of QAOA circuits to reduce gate counts, either by thresholding coupling coefficients or aligning with the processor's qubit topology. This truncation maintains performance while improving experimental feasibility. The paper also generalizes QAOA as a cost-restricted uniform sampling (CRUS) oracle, providing a benchmark for evaluating QAOA performance in large-scale problems. The CRUS framework allows uniform sampling within specific cost intervals, facilitating comparisons with classical methods like semi-definite programming (SDP).

Experimental validation on the IBM Eagle processor for problem sizes up to 64×64 demonstrates the superiority of QAOA-MV over standard QAOA, with error mitigation techniques further enhancing performance. The results show that QAOA-MV reduces the problem dimension by at least ($n/4$) without errors, highlighting its practical potential. The study also explores the trade-offs between truncation, gate counts, and theoretical performance, offering insights into optimizing QAOA for real-world applications.

The paper concludes by discussing open challenges, such as extending the method to higher-order modulations and optimizing QAOA angles for expected bit errors. The authors emphasize the need for future research to explore the scalability of QAOA-MVSIC for larger systems and the integration of advanced error mitigation techniques. Overall, this work represents a significant step toward practical quantum-enhanced solutions for MIMO detection, bridging the gap between theoretical quantum algorithms and their implementation on current hardware.

3.4. Extreme Under Sampling Conditions and Challenges

CS has emerged as a powerful framework for signal acquisition and reconstruction, particularly in resource-constrained environments such as underwater applications. In addition, it should theoretically guarantee the recovery of sparse signal when the number of measurements m exceeds the signal's sparsity parameter k. In practice, the challenges of extreme undersampling include inaccurate signal recovery and increased computational complexity. While existing studies attempted CS in various fields most

of them do not cover undersampling and do not work on real-word applications. This section discusses two studies that highlight limitations and challenges encountered in undersampling CS scenarios: one by F. Y. Wu et al. (2018)'s work on underwater acoustic signal reconstruction and the other one is node locatization in underwater sensor networks written by S. Wang et al. (2019).

F. Y. Wu et al. (2018) presented a CS application for underwater acoustic signals that are inherently non-sparse in the time domain. In the study the signals were converted to a sparse representation using the discrete cosine transform (DCT). In addition an optimized measurement matrix was used. Finally, the approximated l_0 (AL0) norm-based reconstruction algorithm was used to reconstruct signals in underwater wireless sensor networks (UWSNs). By doing so, authors aimed to increase energy efficiency and ensure accurate signal recovery.

The authors used measurements in their simulations where $n = 100$ and $m = 40, 50, \dots, 80$ were varied. Their results show that reconstruction accuracy, measured by SNR and Structural SIMilarity index (SSIM), increases as m increases. Furthermore, the AL0 method is concluded to be a practical solution for UWSNs due to its computational complexity. However, the case of $m < k$ is not explicitly examined in the paper.

In paper written by S. Wang et al. (2019) a range-free node localization algorithm is developed for underwater acoustic sensor networks (UASNs). This work aims to reduce energy consumption and hardware costs. Underwater challenges include signal delay and node mobility. To overcome these challenges, authors combined hop-count-based localization with CS. This not only increases signal accuracy but also eliminates the need for expensive ranging equipment.

The sparsity k in this context arises from the spatial correlation between sensor nodes, where only a few nearby beacon nodes significantly influence the position estimation of an unknown node. The authors implicitly assume that the hop-count vectors are sparse in the spatial domain, as distant beacons contribute minimally to the localization of a given unknown node. However, the paper does not explicitly quantify the sparsity level k or analyze its impact on the required number of measurements m. The CS framework is applied to reconstruct the sparse correlation coefficients between unknown nodes and beacon nodes, but the relationship between m and k—critical for

CS performance—is not discussed. This leaves open questions about the theoretical recovery in the case of $m < k$ which can lead to underdetermined systems and poor localization.

The measurement process involves creating a Gaussian sensing matrix to compress hop-count information and reduce communication overhead. The authors evaluate the algorithm's performance under varying compression ratios. Their simulations demonstrate that higher ratios improve accuracy but at the cost of increased energy consumption.

Although the paper presents CS-based localization method for UASNs it leaves open questions about the extreme undersampling case and computational complexity.

4. CHAPTER: SDP-MVRSIC RECONSTRUCTION ALGORITHM

The Semidefinite Programming with Majority Voting and Recursive Succesive Interference Cancellation (SDP-MVRSIC) algorithm represents a new approach to solving the challenging problem of BCS in extreme undersampling scenarios. In this scenario, number of measurements m is smaller than the number of non-zero elements t in the sparse binary signal $\boldsymbol{x} \in \{-1,1\}^n$. This algorithm combines semidefinite programming (SDP) relaxation with majority voting (MV) and recursive successive interference cancellation (RSIC) to recover the signal. The decoding process is managed by the vector $d_{SIC} = [d_1, \dots, d_L]$, where the total signal length n equals the sum of these partial decoding lengths plus an additional term d_{LP} for the final Linear Programming (LP) stage. The algorithm implements a recursive tree structure, where at each *i*-th decoding step, r_j SDP sampling attempts are made according to the predefined vector $r_{SDP} = [r_1, \dots, r_L]$. This structure generates $N_r \equiv \prod_{j=1}^{L} r_j$ potential solution combinations, represented as rows in the matrix $\widehat{\boldsymbol{X}}_{trials}$. MV is applied both at intermadiate steps and finally across all candidate solutions in $\widehat{\boldsymbol{X}}_{trials}$ to produce the estimate $\widehat{\boldsymbol{x}}$. Each candidate solution undergoes *L* partial decoding stages: Randomized SDP sampling, Selection of N_m lowest-cost strings, MV accross bits, and SIC application. The residual signal segment of length d_{LP} is subsequently recovered via LP, which demonstrates strong performance when the measurement condition $m > r_{LP}n$ is satisfied, with r_{LP} approaching 0.5 as n increases based on study written by O. L. Mangasarian et al (2011). The cost function for the system $\boldsymbol{y} = \boldsymbol{H}\boldsymbol{x}$ is defined as:

$$C(\widehat{\boldsymbol{x}}) = \|\boldsymbol{y} - \boldsymbol{H}\widehat{\boldsymbol{x}}\|_2^2 \tag{6}$$

where $\boldsymbol{x}$ is $t \times 1$ vector and $\boldsymbol{H}$ is $n \times t$ matrix. The steps of the algorithm for obtaining a single candidate solution is explained in remaining part of this chapter.

4.1. Randomized SDP Relaxation

At the core of the SDP-MVRSIC algorithm lies the reformulation of (2) into a tractable convex optimization framework (7) through semidefinite programming which

motivated by high performance of decoding with a cost-based approach in maximum-likelihood (ML) problem in paper by B. Gulbahar (2025):

$$\min_{\hat{\boldsymbol{x}}} \ \|\boldsymbol{y} - \boldsymbol{H}\hat{\boldsymbol{x}}\|_2^2 \tag{7}$$

$$\min_{\boldsymbol{S}} tr(\boldsymbol{Q}\boldsymbol{S}) \ \ subject\ to\ \boldsymbol{S} \geq 0\ and\ S_{i,i} = 1\ for\ i \in [1, n+1] \tag{8}$$

where $tr(.)$ is the trace operator, $\boldsymbol{S} = \boldsymbol{z}\boldsymbol{z}^T$ refers to rank-1 matrix, $\boldsymbol{S} \geq 0$ enforces the positive semi-definiteness and $\boldsymbol{Q}$ is defined as $(n+1) \times (n+1)$ matrix:

$$\boldsymbol{Q} = \begin{bmatrix} \boldsymbol{H}^T\boldsymbol{H} & -\boldsymbol{H}^T\boldsymbol{y} \\ -\boldsymbol{y}^T\boldsymbol{H} & 0 \end{bmatrix} \tag{9}$$

The solution $\widehat{\boldsymbol{S}}$ allows to generate N_s random sample vectors from a multivariate Gaussian distribution $\mathcal{N}(0, \widehat{\boldsymbol{S}})$ having the covariance matrix $\widehat{\boldsymbol{S}}$. Random sample vectors are quantized with $f_{sign}(.)$ operator while excluding the last element. For each candidate sample satisfying number of non-zero elements lower than corresponding t.

This randomization introduces diversity in candidate solutions, enhancing the robustness of the recovery process.

4.2. Majority Voting

Majority Voting (MV) operates as a statistical decision rule that minimizes the expected bit error rate by assigning the most frequent bit values. At each *i*-th decoding step, we operate on a problem formulation $\boldsymbol{y}_{rev} = \boldsymbol{H}_{rev}\boldsymbol{x}_{rev}$, where $\boldsymbol{H}_{rev} \in \mathbb{R}^{n \times t}$ is the current measurement matrix and $\boldsymbol{x}_{rev} \in \{-1,1\}^t$ represents the remaining undecoded bits. The original signal indices corresponding to the $\boldsymbol{x}_{rev}$ are maintained in set $\boldsymbol{S} = \{S_l | l \in [1,t], S_l \in [1,n]\}$, ensuring $x_{rev,l} = x_{S_l}$.

From the randomized SDP sampling stage, we generate N_s candidate vectors $\{\boldsymbol{z}_j\}$, each of length t. These candidates are evaluated using the cost function $C(\boldsymbol{z}_j) = \left\|\boldsymbol{y}_{rev} - (\boldsymbol{H}_{rev}\boldsymbol{z}_j)\right\|_2^2$ and sorted by ascending cost, producing an ordered index set M. For bit position l, we compute the aggregate counts $|c_l| = \left|\sum_{j=1}^{N_m} z_{M_i,l}\right|$, which quantifies the agreement among the top N_m lowest-cost candidates.

The decoding proceeds by:

1. Sorting all $|c_l|$ values in descending order,

2. Selecting the first d_i indices $V \equiv \{V_1, \dots, V_{d_i}\}$,
3. Determining the decoded bits: $\hat{x}_{part,j} = f_{sign}\left(c_{V_j}\right)$ for $j \in [1, d_i]$.

The indices of decoded bits are tracked in $\boldsymbol{S}(\boldsymbol{V}) = \left\{S_{V_1}, \dots, S_{V_{d_i}}\right\}$, while the remaining undecoded indices are maintained in $\boldsymbol{S}(\overline{\boldsymbol{V}})$, where $\overline{\mathbf{V}} = \{1, \dots, t\} \backslash \mathbf{V}$ denotes the complement of $\mathbf{V}$.

4.3. Successive Interference Cancellation (SIC)

The Successive Interference Cancellation (SIC) in the SDP-MVRSIC algorithm plays a pivotal role in dynamically reducing the problem dimensionality while mitigating error propagation. SIC operates iteratively removing the contribution of decoded signal components from the measurement vector. At the i-th decoding step, the algorithm estimates a segment $\hat{\boldsymbol{x}}_{part}$ of length d_i via majority voting. The residual measurement vector $\boldsymbol{y}_{rev}$ and revised measurement matrix $\boldsymbol{H}_{rev}$ are then computed as follows:

$$\begin{aligned} \boldsymbol{y}_{rev} &= \boldsymbol{y} - \left(\boldsymbol{H}_{\boldsymbol{V}} \hat{\boldsymbol{x}}_{\boldsymbol{S}(\boldsymbol{V})}\right), \\ \boldsymbol{H}_{rev} &= \boldsymbol{H}_{\overline{\boldsymbol{V}}}, \\ \boldsymbol{S}_{rev} &= \boldsymbol{S}(\overline{\boldsymbol{V}}), \end{aligned} \tag{10}$$

where $\boldsymbol{V} = \left\{V_1, \dots, V_{d_i}\right\}$ denotes indices of the decoded bits, $\overline{\boldsymbol{V}} = \{1, \dots, t\} \backslash \boldsymbol{V}$ represents the remaining undecoded indices, $\boldsymbol{H}_{\boldsymbol{V}}$ and $\boldsymbol{H}_{\overline{\boldsymbol{V}}}$ are submatrices of $\boldsymbol{H}$ with columns indexed by $\boldsymbol{V}$ and $\overline{\boldsymbol{V}}$, respectively.

4.4. Linear Programming

In the final segment, the algorithm employs LP to recover the remaining bits. The LP solves the following optimization problem:

$$\min_{\boldsymbol{x}, \delta} \delta \ \ subject\ to\ \boldsymbol{H}\boldsymbol{x} = \boldsymbol{y}, -\delta \mathbf{1} \leq \boldsymbol{x} \leq \delta \mathbf{1}, \delta \geq 0, \tag{11}$$

where $\boldsymbol{x} \in \mathbb{R}^n$ is the signal to be recovered, $\boldsymbol{H} \in \mathbb{R}^{m \times n}$ is the measurement matrix, $\boldsymbol{y} \in \mathbb{R}^m$ is the measurement vector, and δ is the slack variable that bounds the signal values. This formulation converts the l_∞-norm minimization into a standard linear program, solvable via using `linprog` tool in MATLAB based on simplex solver. After solving the LP problem (11), obtained $\boldsymbol{x}^{LP}$ is quantized to binary values using the sign function:

$$\hat{\boldsymbol{x}}_{LP} = f_{sign}(\boldsymbol{x}^{LP}), where\ f_{sign}(z) = \begin{cases} +1\ if\ z \geq 0, \\ -1\ otherwise. \end{cases} \quad (12)$$

LP part involves $n + 1$ variables and $m + 2n$ linear constraints.

5. CHAPTER: SDP WITH SPARSE MEASUREMENTS

The SDP with Sparse Measurements approach presents a structured method for recovering signals from compressed measurements. The algorithm begins by taking as input the sparse measurement vector $\boldsymbol{y}$ and measurement matrix $\boldsymbol{H}$, then initializes the problem dimension n, sparsity parameter t, and solution vector $\boldsymbol{x}$.

Important feature of this approach is the construction of the sparse binary measurement matrix $\boldsymbol{H} \in \mathbb{R}^{m \times n}$ where most elements are zero. Sparse measurement matrices offer practical advantages in compressed sensing, particularly in reducing computational complexity and storage requirements compared to dense Gaussian matrices which are mentioned in W. Wang et al.'s (2010) work. However, it comes at a potential cost: sparse matrices may require more number of measurements for exact signal recovery due to its weaker statistical guarantees. In our study, we use this sparsity pattern to enable computational efficiency while recovering signal exactly.

Sparse measurements are obtained by using these sparse measurement matrix. The objective function which addresses challenges of non-convex optimization for signal recovery is reformulated as follows:

$$\min_{z,\boldsymbol{Z}} \sum_{i=1}^{n} z_i - tr(\boldsymbol{Z}) \tag{13}$$

where $tr(.)$ is the trace operator. This formulation is directly inspired by polynomial optimization problem proposed by S. M. Fosson et al. (2019). In this problem, minimizing of $\sum_{i=1}^{n}(x_i - x_i^2)$ under binary constraints naturally leads to solutions in $\{0,1\}^n$. By transforming the polynomial objective function into an SDP framework, it protects the fundamental properties of binary implementation and it allows us to use convex optimization tools.

This formulation balances two conditions: sparsity via the linear term $\sum_{i=1}^{n} z_i$, and the validity of the semidefinite relaxation via the trace term $-tr(\boldsymbol{Z})$. The linear term $\sum_{i=1}^{n} z_i$ penalizes deviations from binary values (i.e., $z_i \in \{-1,1\}$). By minimizing this

term, the algorithm encourages the variables z_i to approach their bounds. However, since this term alone can lead to unconstrained solutions we also add the trace term.

The trace term $-tr(\boldsymbol{Z})$ serves as a counterbalance, effectively maximizing the sum of the diagonal elements of the matrix $\boldsymbol{Z}$. This is important because in semidefinite relaxations, $\boldsymbol{Z}$ is often a representation of a rank-1 matrix (e.g., $\boldsymbol{Z} = \boldsymbol{z}\boldsymbol{z}^T$ in an ideal case). The linear term drives sparsity or discreteness, while the trace term preserves the geometric and algebraic integrity of the semidefinite formulation.

Here, $tr(\boldsymbol{Z})$ simplifies to $\sum_{i=1}^{n} z_i^2$, this expression is maximized when z_i takes values in $\{-1, 1\}$, as $z_i - z_i^2$ reaches its maximum value of zero at these points and is negative elsewhere.

The constraints are defined as the following:

$$\begin{gathered} \boldsymbol{y} = \boldsymbol{H}\boldsymbol{z} \\ \boldsymbol{Z} \geq 0 \\ diag(\boldsymbol{Z}) = \mathbf{1} \\ -1 \leq z_i \leq 1, i = 1, \dots, n \end{gathered} \tag{14}$$

The equality constraint ensures that the solution $\boldsymbol{z}$ is consistent with the sparse measurements $\boldsymbol{y}$, while the $\boldsymbol{Z} \geq 0$ guarantees the semidefiniteness condition of the matrix $\boldsymbol{Z}$. The bounds $-1 \leq z_i \leq 1$ prevent the variables from deviating from realistic values.

Chapter 7 evaluates the performance of SDP with sparse measurement method and the proposed SDP-MVRSIC algorithm against the state-of-the-art methods in the literature.

6. CHAPTER: COMPUTATIONAL COMPLEXITY OF SDP-MVRSIC ALGORITHM

This section provides a comprehensive analysis of the SDP-MVRSIC algorithm's complexity characteristics, examining the contribution of each component and their collective impact on overall performance.

The algorithm's complexity is fundamentally determined by its segment based architecture where the problem size is reduced through SIC. At each decoding stage i, the algorithm operates on a reduced problem size $t_i = n - \sum_{j=1}^{i-1} d_j$, where d_j represents the number of bits decoded in previous steps. This progressive reduction is crucial for managing computational load while maintaining recovery performance.

As can be seen in Table 1, the SDP phase dominates the computational burden, particularly in early iterations when t_i is largest. Solving the SDP problem in (8) incurs $O\left(t_i^{3.5}\right)$ complexity. This is compounded by the randomized sampling step, which generates N_s candidate solutions from a Gaussian distribution $N\left(0, \widehat{\boldsymbol{S}}\right)$, adding $O(N_s t_i^2)$ operations. The sampling process includes a sparsity check that discards candidates exceeding the target sparsity by a factor Δ (typically 1.1), adding negligible overhead while improving solution quality.

The MV stage introduces complementary costs: evaluationg N_s candidates against the measurement constraints requires $O(N_s t_i^2)$ operations, while sorting and aggregating bit decisions across the N_m lowest-cost candidates contribute $O(N_s \log N_s) + O(N_m t_i)$ complexity.

The final linear programming step, applied once to the residual problem of size d_{LP}, exhibits $O(d_{LP}^3)$ complexity, though its impact is mitigated by the progressive dimensionality reduction enabled by SIC.

Table 6.1. Single-Step Complexity of SDP-MVRSIC $(m \times t)$

Task	Complexity
SDP	$O(t^{3.5} + N_s\, t^2)$
Cost calculation	$O(N_s\, t^2)$
LP	$O(t^3)$
Sorting N_s samples	$O(N_s\, \log N_s)$
MV counting	$O(N_m\, t)$
MV sorting	$O(t\, \log t)$

Source: Author

The recursive structure of SDP-MVRSIC introduces a combinatorial through its attempt limits $r_{SDP} = [r_1, \dots, r_L]$. The total complexity scales with the product of attempts across L layers $(N_r = \prod_{j=1}^{L} r_j)$. For N_s, $N_m \sim O(n)$, the worst-case complexity is bounded by:

$$\sum_{i=1}^{L} O\left(\left(t_i^{3.5} + nt_i^2\right)\prod\nolimits_{j=1}^{i} r_j\right) = O(n^{c_o}) < O(n^{3.5} L N_r) \tag{15}$$

For $n = 128$, this empirically ranges between $O(n^{3.83})$ and $O(n^{5.86})$, depending on d_{SIC} and r_{SDP}.

After obtaining each possible solution, noiseless case allows to verify whether it is successfully recovered by achieving $\|\boldsymbol{y} - \boldsymbol{H}\hat{\boldsymbol{x}}_{trial}\|_2^2$ is 0. Therefore, we terminate algorithm earlier to increase its computational efficiency.

The complexity analysis varies for the SDP-MVRSIC (type a, b, c) methods due to the different parameter choices. For the SDP-MVRSIC-c configuration (with lower trial limits), the average complexity is calculated as $\approx O(n^{3.8})$, and signal recovery begins at $m/k > 0.785$. In contrast, the SDP-MVRSIC-a configuration (with higher trial limits) begins recovery at $m/k > 0.6875$ but has a complexity of $\approx O(n^5)$.

This analysis demonstrates that SDP-MVRSIC's polynomial-time operations increase the complexity, resulting in improved performance extreme undersampling. The algorithm is promising for applications where measurement constraints are high but compational resources are available.

7. CHAPTER: NUMERICAL SIMULATIONS

The simulations in this study evaluate the performance of the proposed SDP-MVRSIC and SDP with sparse measurements methods by comparing its exact recovery rate (r_e), bit-error rate (BER), and computational complexity with existing binary compressed sensing (BCS) methods, weak threshold (2010), MMSE-OMP (2016), RW-RWR (2018), and POP (2019). For the simulations, we perform 100 experiments for each case while $N_s = 16384$ and $N_m = 16$. The signal length of $n = 128$ was selected, with sparsity level $s = k/n$ and m/n are both chosen in the set $[0.125, 0.5]$.

7.1. Recovery Performance of SDP with Sparse Measurements

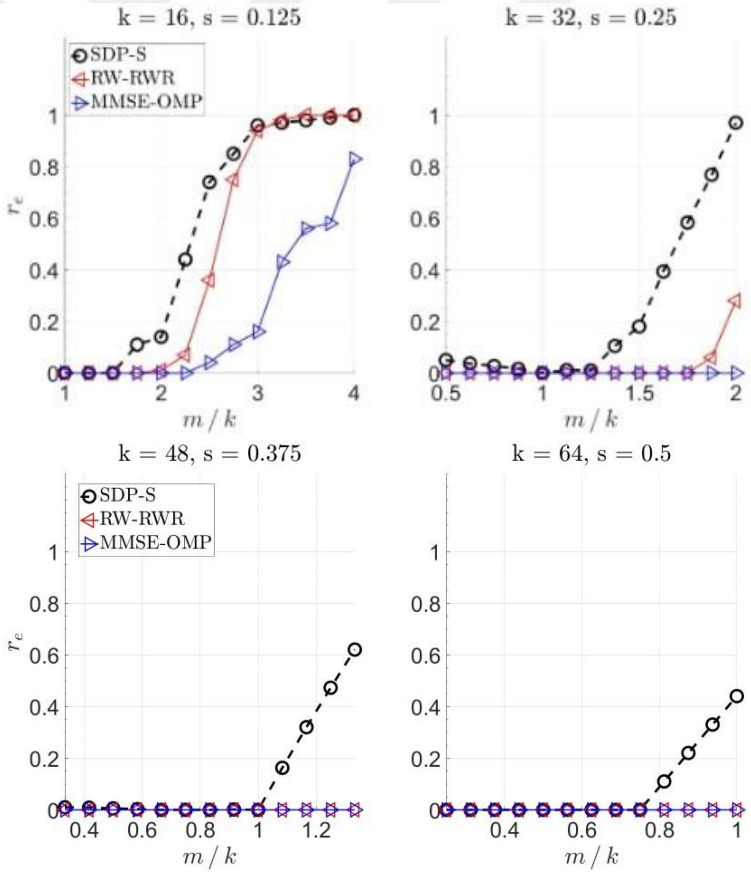

Figure 7.1. SDP-S, RW-RWR (2018) and MMSE-OMP (2016) performances are compared for k = 16, 32, 48 and 64 for exact recovery rate for varying m/k.

Source: Author

The exact recovery performance comparison reveals significant differences between the three algorithms across various sparsity regimes. In Figure 7.1 the proposed SDP-S (SDP with sparse measurements) method demonstrates remarkable effectiveness in extreme undersampling conditions, particularly when the measurement-to-sparsity ratio (m/k) falls below 1.5. For $k = 32$ $(s = 0.25)$, SDP-S achieves near-perfect recovery $(r_e > 0.9)$ at $m/k \approx 2$, while RW-RWR (2018)'s recovery performance is $r_e \approx 0.37$ and MMSE-OMP (2016) is 0.

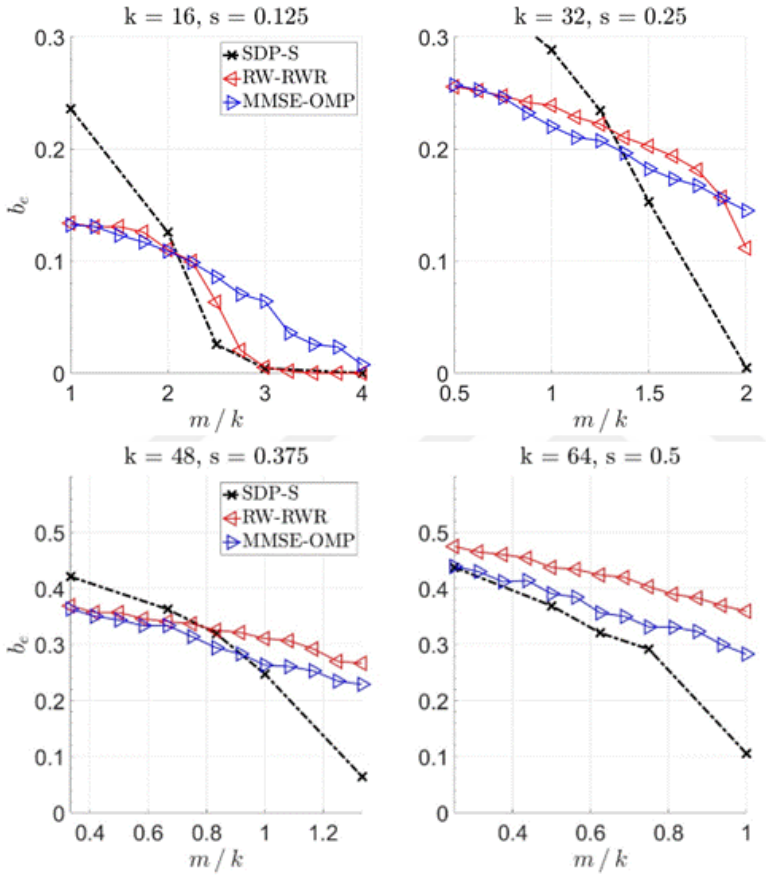

Figure 7.2. SDP-S, RW-RWR (2018) and MMSE-OMP (2016) performances are compared for k = 16, 32, 48 and 64 for bit error rate for varying m/k.

Source: Author

As sparsity increases to $k = 64$ $(s = 0.5)$, while all algorithms show degraded performance due to the increased problem complexity, SDP-S achieves $r_e \approx 0.41$ at $m/k = 1$. The performance hierarchy remains consistent across all tested sparsity

levels, with SDP-S outperforming RW-RWR (2018), which in turn surpasses MMSE-OMP (2016).

Figure 7.2 demonstrates that when the signal is not perfectly recovered, the SDP-S method exhibits a less severe degradation in bit error rate (BER) performance compared to RW-RWR (2018) and MMSE-OMP (2016) as the sparsity ratio decreases. For instance, at $k = 32$ ($s = 0.25$), when the m/k ratio increases from ≈ 1 to ≈ 2, the BER for SDP-S drops sharply from 0.2883 to 0.00455, whereas RW-RWR (2018) only improves from 0.24 to 0.1103, and MMSE-OMP (2016) declines from 0.2256 to 0.1372. While the BER increases for all three methods as sparsity rises, SDP-S consistently outperforms the other two at low m/k ratios. These results suggest that SDP-S is particularly advantageous in scenarios with high sparsity but limited measurements, making it a more robust choice under extreme undersampling conditions compared to other two methods.

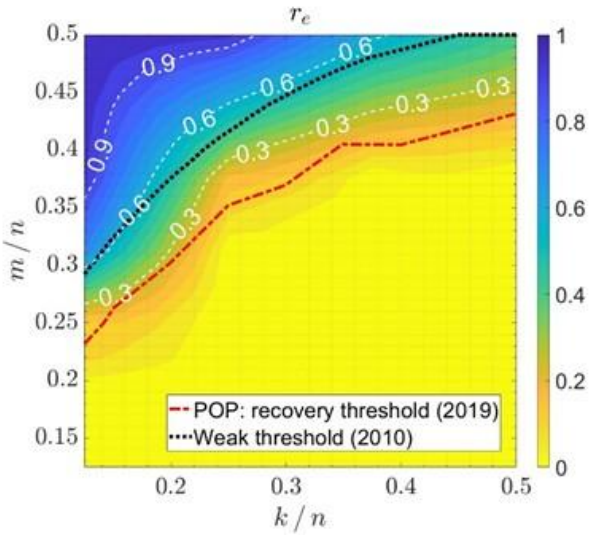

Figure 7.3. SDP-S for varying $k/n, m/n \in [0.125, 0.5]$ compared with thresholds in POP (2019), Weak threshold (2010) for exact recovery rate.

Source: Author

In Figure 7.3, the red dashed line marks the recovery threshold for the POP (2019) method (left side indicates recoverable signals), while the black dashed line represents the weak threshold (2010) boundary. For our proposed SDP-S algorithm, signal recovery begins beyond the yellow region's boundary, extending into the blue-shaded area (leftward direction). This demonstrates that SDP-S successfully recovers certain signals that remain unrecoverable by the other two methods.

The proposed SDP-S algorithm demonstrates a robust and versatile performance profile across all evaluation metrics, establishing itself as a significant advancement in binary compressed sensing. As evidenced by the exact recovery rate (r_e in Figure 7.1), BER, and threshold comparison analyses, SDP-S consistently outperforms existing methods in the most challenging operational regimes while maintaining competitive performance across all tested conditions. The algorithm's most notable strength lies in its ability to achieve successful recovery in extreme undersampling scenarios ($m/k < 1$) where both the polynomial optimization approach (POP, 2019) and the weak threshold (2010) methods fail completely.

7.2. Recovery Performance of SDP-MVRSIC and Computational Complexity Analysis

The performance of SDP-MVRSIC was evaluated through simulations with signal length $n = 128$, where sparsity ratio $s = k/n$ and measurement ratio m/k were both varied between $[0.125, 0.5]$. Three parameter settings (a, b, c) were tested to analyze the complexity-performance trade-off, with $\log_n N_r$ values of 5.86, 4.74 and 3.83 corresponding to increasing complexity levels. For each case, $M = 100$ experiments were conducted with $N_s = 16384$ samples and $N_m = 16$ majority voting candidates.

In Figure 7.4, exact recovery rates (r_e) were compared against RW-RWR (2018) and MMSE-OMP (2016) methods across different sparsity levels. For $s = 0.125$ ($k = 16$), $SDP - MVRSIC_a$ achieved recovery at $m/k \geq 1.5$ while other methods required $m/k \geq 3$. At higher sparsity ($s = 0.25 - 0.5$), SDP-MVRSIC demonstrated superior performance in extreme undersampling ($m/k < 2$), with $SDP - MVRSIC_c$ showing $r_e \approx 0.2$ at $m/k \approx 1.5$, 1 and 0.85 for $s = 0.25$, 0.375 and 0.5 respectively, where conventional methods failed completely.

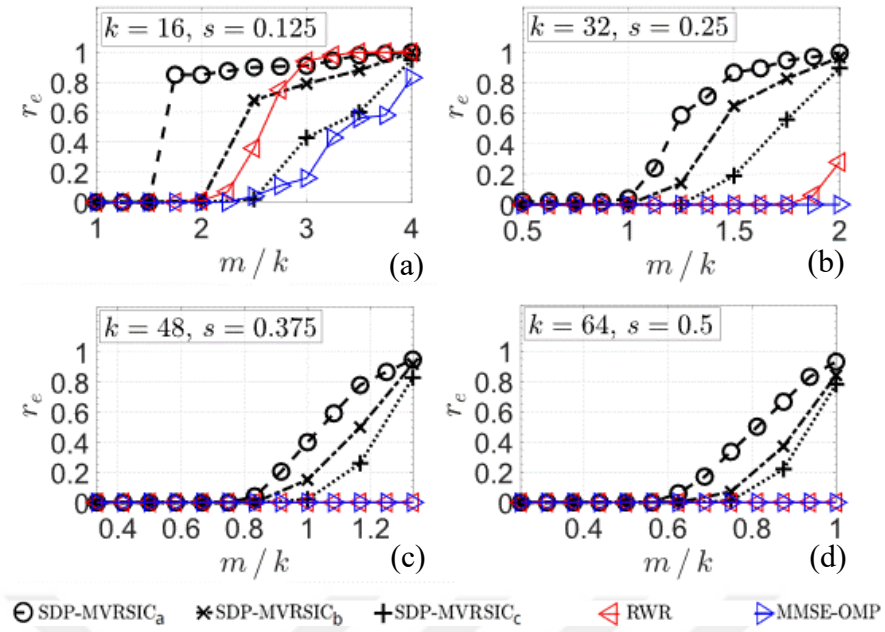

Figure 7.4. SDP-MVRSIC for types a, b and c, RWR (2018) and MMSE-OMP (2016) performances are compared for k = 16, 32, 48 and 64 in Figs. 7.4(a), (b), (c) and (d) for exact recovery rate.

Source: Author

BER performance comparisons (Figure 7.5) revealed that $SDP - MVRSIC_b$ outperformed RWR (2018) and MMSE-OMP (2016) for $s \geq 0.25$, achieving near-zero b_e at $m/k \approx 2$, 1.3 and 1 for $s = 0.25$, 0.375 and 0.5 respectively.

As shown in Figure 7.6 the computational complexity was analyzed through c_o values calculated from actual operation counts, showing that increased complexity ($c_o \in$ [4.2,5.5] for type-a) enabled recovery in $m < k$ regimes, while type-c ($c_o \in$ [3.7,3.85]) approached POP (2019) thresholds with lower complexity.

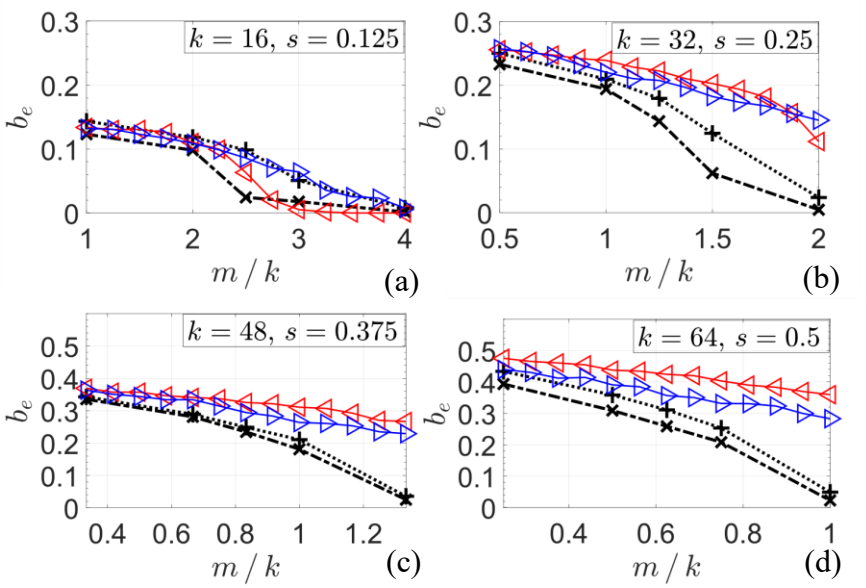

Figure 7.5. SDP-MVRSIC for types a, b and c, RWR (2018) and MMSE-OMP (2016) performances are compared for k = 16, 32, 48 and 64 in Figs. 7.5(a), (b), (c) and (d) for bit error rate.

Source: Author

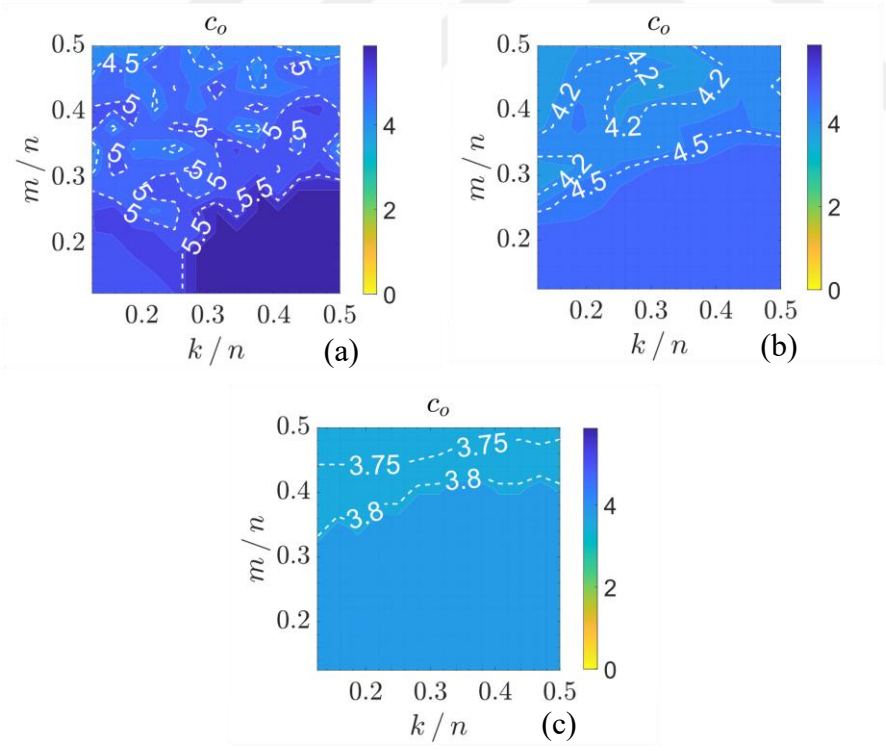

Figure 7.6. SDP-MVRSIC with types a, b and c for varying $k/n, m/n \in [0.125, 0.5]$ for computational complexity in Figs. 7.6(a), (b) and (c).

Source: Author

Figure 7.7 presents a comparative analysis of the exact recovery rates achieved by SDP-MVRSIC across its three parameter configurations (types a, b, and c) against established theoretical thresholds by weak threshold (2010) and POP (2019). The results are plotted for varying sparsity ratios (k/n) and measurement ratios (m/n), both ranging from 0.125 to 0.5. This visualization effectively captures the algorithm's performance across different undersampling regimes and computational complexity levels.

Particularly noteworthy is the performance of type-a configuration (highest complexity), which achieves successful recovery in the most challenging undersampled cases ($m/n < k/n$). The type-b configuration shows a balanced trade-off between complexity and performance, while type-c maintains competitive recovery rates at significantly reduced computational cost.

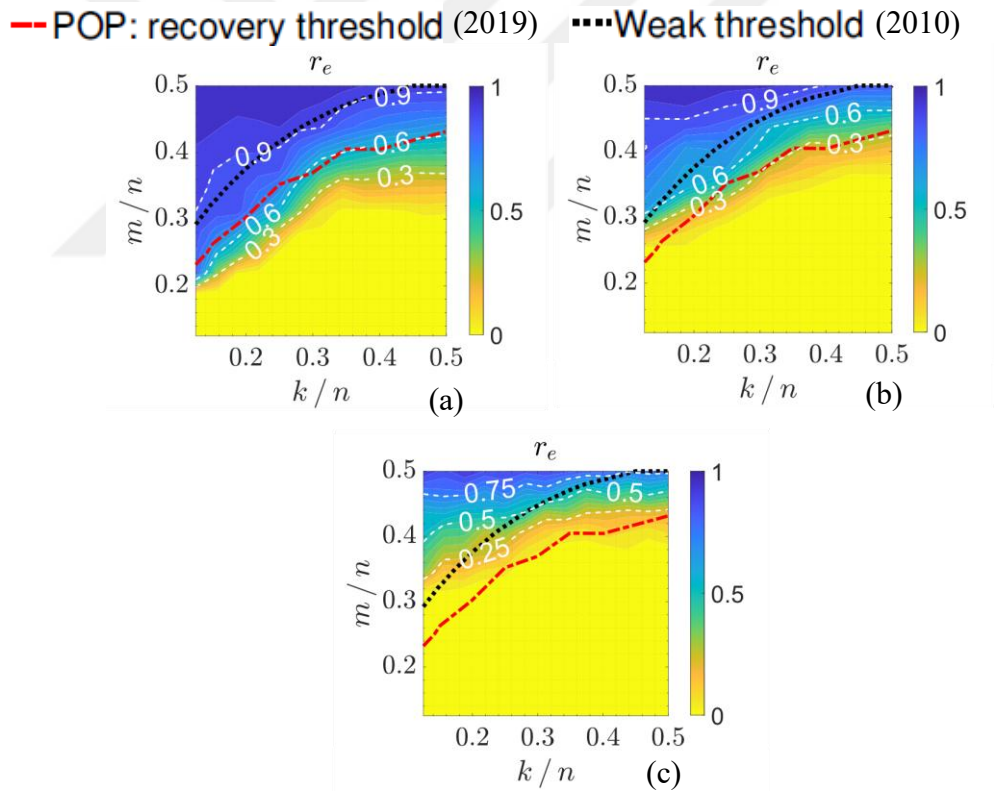

Figure 7.7. SDP-MVRSIC with types a, b and c for varying $k/n, m/n \in [0.125, 0.5]$ compared with thresholds in papers by S. M. Fosson et al. (2019), M. Stojnic (2010) for exact recovery rate in Figs. 7.6(a), (b) and (c).

Source: Author

The simulations show that our method SDP-MVRSIC recovers signal in previously unreachable undersampling regimes compared to weak threshold (2010), MMSE-OMP (2016), RW-RWR (2018) and POP (2019). The method's performance scales with computational complexity, with type-a and b configurations exceeding existing methods and type-c approaches the performance of POP (2019).

8. CHAPTER 8: CONCLUSION

In conclusion, our method SDP-MVRSIC presents a new approach to BCS in severely undersampled regimes ($m < 2k$), offering a tunable trade-off between computational complexity and recovery performance. By combining semidefinite programming (SDP), majority voting (MV), and recursive successive interference cancellation (SIC), the algorithm achieves exact recovery in cases where conventional methods fail, particularly when $m < k$. The complexity scales polynomially with signal length ($O(n^{3.83})$ to $O(n^{5.86})$ for $n = 128$), making it feasible for practical applications while outperforming existing techniques such as RW-RWR (2018) and MMSE-OMP (2016).

In addition to SDP-MVRSIC, other algorithm we proposed the SDP-S also demonstrates competitive performance, particularly in moderate undersampling scenarios. While it lacks the recursive structure of SDP-MVRSIC, SDP-S achieves reasonable recovery rates with lower computational complexity, making it suitable for cases where complexity must be minimized. However, its performance decreases in extreme undersampling ($m < k$), where SDP-MVRSIC's recursive structure successfully recover the signal.

9. FUTURE WORK

SDP-MVRSIC offers an adjustable trade-off between computational complexity and performance, particularly for extreme undersampling BCS problems where $m < k$. However, there remain several open challenges to enhance the proposed design:

- Develop an optimization technique to tune r_{SDP} and d_{SIC} for a given n (where $L \ll n$) while achieving the desired exact recovery rate (r_e) or bit error rate (b_e).
- Analyze the scaling behavior of computational complexity (c_o) and its dependence on n for a fixed target r_e, using optimized r_{SDP} and d_{SIC} parameters.
- Investigate the performance of SDP-MVSIC in scenarios involving noisy BCS.
- Explore alternative sampling methods, such as cost-based approaches, including quantum algorithms such as QAOA (as referenced in paper by B. Gulbahar (2025)). These methods may offer lower computational costs compared to SDP-based sampling while maintaining promising performance.

10. CODE AVAILABILITY

The complete MATLAB implementation of our SDP-MVRSIC decoder is openly available as a Compute Capsule on Code Ocean (July 23, 2025), with corresponding simulation results for exact recovery hosted on IEEE DataPort (July 23, 2025).

11. REFERENCES

Donoho, D. L. (2006). Compressed sensing. *IEEE Transactions on information theory, 52*(4), 1289-1306. http://dx.doi.org/10.1109/TIT.2006.871582

Candès, E. J., Romberg, J., & Tao, T. (2006). Robust uncertainty principles: Exact signal reconstruction from highly incomplete frequency information. *IEEE Transactions on information theory*, *52*(2), 489-509. http://dx.doi.org/10.1109/TIT.2005.862083

Candès, E. J., & Tao, T. (2005). Decoding by linear programming. *IEEE transactions on information theory*, *51*(12), 4203-4215. http://dx.doi.org/10.1109/TIT.2005.858979

Chen, S. S., Donoho, D. L., & Saunders, M. A. (2001). Atomic decomposition by basis pursuit. *SIAM review*, *43*(1), 129-159. http://dx.doi.org/10.1137/S1064827596304010

Candès, E. J., Wakin, M. B., & Boyd, S. P. (2008). Enhancing sparsity by reweighted ℓ1 minimization. *Journal of Fourier analysis and applications*, *14*(5), 877-905. https://doi.org/10.48550/arXiv.0711.1612

Stojnic, M. (2010, June). Recovery thresholds for ℓ 1 optimization in binary compressed sensing. In *2010 IEEE International Symposium on Information Theory* (pp. 1593-1597). IEEE. http://dx.doi.org/10.1109/ISIT.2010.5513435

Nakarmi, U., & Rahnavard, N. (2012, October). BCS: Compressive sensing for binary sparse signals. In *MILCOM 2012-2012 IEEE Military Communications Conference* (pp. 1-5). IEEE. http://dx.doi.org/10.1109/MILCOM.2012.6415872

Baraniuk, R., Davenport, M., DeVore, R., & Wakin, M. (2008). A simple proof of the restricted isometry property for random matrices. *Constructive approximation*, *28*(3), 253-263. http://dx.doi.org/10.1007/s00365-007-9003-x

Hajji, Z., Amis, K., & El Bey, A. A. (2020). Iterative receivers for large-scale MIMO systems with finite-alphabet simplicity-based detection. *IEEE Access*, *8*, 21742-21758. http://dx.doi.org/10.1109/ACCESS.2020.2969710

Hayakawa, R., & Hayashi, K. (2017). Convex optimization-based signal detection for massive overloaded MIMO systems. *IEEE Transactions on Wireless Communications*, *16*(11), 7080-7091. http://dx.doi.org/10.1109/TWC.2017.2739140

Pati, Y. C., Rezaiifar, R., & Krishnaprasad, P. S. (1993, November). Orthogonal matching pursuit: Recursive function approximation with applications to wavelet decomposition. In *Proceedings of 27th Asilomar conference on signals, systems and computers* (pp. 40-44). IEEE. http://dx.doi.org/10.1109/ACSSC.1993.342465

Sparrer, S., & Fischer, R. F. H. (2016). MMSE-based version of OMP for recovery of discrete-valued sparse signals. *Electronics Letters*, *52*(1), 75-77. http://dx.doi.org/10.1049/el.2015.0924

Fosson, S. M. (2018, October). Non-convex approach to binary compressed sensing. In *2018 52nd Asilomar Conference on Signals, Systems, and Computers* (pp. 1959-1963). IEEE. http://dx.doi.org/10.1109/ACSSC.2018.8645293

Fosson, S. M., & Abuabiah, M. (2019). Recovery of binary sparse signals from compressed linear measurements via polynomial optimization. *IEEE Signal Processing Letters*, *26*(7), 1070-1074. http://dx.doi.org/10.1109/LSP.2019.2919943

Gulbahar, B. (2025). Majority voting with recursive QAOA and cost-restricted uniform sampling for maximum-likelihood detection in massive MIMO. *IEEE Transactions on Wireless Communications*. http://dx.doi.org/10.1109/TWC.2024.3523135

Wu, F. Y., Yang, K., Duan, R., & Tian, T. (2018). Compressive sampling and reconstruction of acoustic signal in underwater wireless sensor networks. *IEEE Sensors Journal*, *18*(14), 5876-5884. http://dx.doi.org/10.1109/JSEN.2018.2839772

Wang, S., Lin, Y., Tao, H., Sharma, P. K., & Wang, J. (2019). Underwater acoustic sensor networks node localization based on compressive sensing in water hydrology. *Sensors*, *19*(20), 4552. http://dx.doi.org/10.3390/s19204552

Mangasarian, O. L., & Recht, B. (2011). Probability of unique integer solution to a system of linear equations. *European Journal of Operational Research*, *214*(1), 27-30. http://dx.doi.org/10.1016/j.ejor.2011.04.010

Wang, W., Wainwright, M. J., & Ramchandran, K. (2010). Information-theoretic limits on sparse signal recovery: Dense versus sparse measurement matrices. *IEEE Transactions on Information Theory*, *56*(6), 2967-2979. http://dx.doi.org/10.1109/TIT.2010.2046199

Abay, E., & Gulbahar, B. (2025, July). Binary signal recovery in extreme undersampling: SDP with majority voting and recursive successive interference cancellation. *Code Ocean Compute Capsule*. Available: https://codeocean.com/capsule/6697740/tree/v1. https://10.24433/CO.0418545.v1

Abay, E., & Gulbahar, B., (2025, July). Binary signal recovery in extreme undersampling: SDP with majority voting and recursive successive interference cancellation. *IEEE Dataport.* https://dx.doi.org/10.21227/fpz6-cx31